

Structures in elastic, vibrational, and dissociative electron attachment cross sections in N₂O near threshold

M Allan and T Skalický

Department of Chemistry, University of Fribourg, CH-1700 Fribourg, Switzerland

Abstract

Absolute differential cross sections were measured at 135° for the elastic and the vibrationally inelastic electron scattering from threshold to 12 eV, with emphasis on the threshold region. In addition, relative dissociative electron attachment spectra were measured from 0.1 to 3.5 eV. Structures of vibrational origin were observed at energies below 1 eV, well below the ²Π shape resonance, in the cross sections for the excitation of vibrational overtones and for dissociative attachment. They are generally narrower and deeper than similar structures in CO₂. The structures are absent when the N≡N stretch is co-excited. The structures are interpreted in terms of vibrational Feshbach resonances supported by a state of the anion where an electron is temporarily loosely bound in a spatially diffuse cloud by a combination of dipolar and polarization forces around a molecule with an excited bending and/or N–O stretch vibration.

1. Introduction

This work extends studies of threshold peaks and near-threshold structures in electron scattering to the weakly polar molecule N₂O. Threshold peaks in vibrational excitation cross sections were originally discovered in the polar molecules hydrogen halides by Rohr and Linder (1976). Cvejanović and Jureta (1989) and Cvejanović (1993) later discovered oscillatory structures very near threshold in HCl, unexpected in view of the large autodetachment width of the s-wave dominated σ^* valence shape resonance. Ehrhardt and co-workers (Knoth *et al* 1989) found similar structures of varying width in HF and identified them as vibrational Feshbach resonances. The threshold peaks and near-threshold structure in hydrogen halides have recently been studied in greater detail both experimentally and theoretically (Allan *et al* 2000, Čížek *et al* 2001, 2002, 2003).

Threshold peaks (Kochem *et al* 1985) and near-threshold structures due to vibrational Feshbach resonances (Allan 2002) were also later observed in the nonpolar polyatomic molecule CO₂. The example of CO₂ shows that a permanent dipole moment is not required—a combination of a polarization force and the fact that the molecule acquires a dipole moment when it is bent appears to be sufficient. Vibrational Feshbach resonances appear to be very common among polyatomic molecules, which often have large polarizabilities and either have permanent dipole moments, or acquire a dipole moment when distorted along a non-totally symmetrical vibrational normal mode. In fact, vibrational Feshbach resonances (called ‘nuclear excited resonances’ at the time) were invoked to explain large capture probabilities for thermal electrons in large molecules like substituted nitrobenzenes (Christophorou *et al* 1984), although individual resonances were not resolved at that time. Sharp structures were found near threshold in elastic and vibrational (Allan 2001, 2003), and the total (Jones *et al* 2002) cross sections in CS₂, but appear to be due primarily to a valence state (shape resonance) of the anion in contrast to the ‘diffuse’ state in the hydrogen halides and CO₂.

N₂O is isoelectronic with CO₂. The average polarizabilities of the two molecules are very similar ($\alpha(\text{N}_2\text{O}) = 20a_0^3$, $\alpha(\text{CO}_2) = 19a_0^3$, Lide (1995), Alms *et al* (1975)). The permanent dipole moment of N₂O is very small (0.16 D, Jalink *et al* (1987)) and nearly irrelevant for electron binding. A more important difference in comparison to CO₂ is that N₂O has a low-lying threshold for dissociative electron attachment, 0.21 eV (Kaufman 1967), which permits study of the vibrational Feshbach resonances in the dissociative electron attachment channel.

Cross sections in N₂O have been studied above about 1 eV both experimentally and theoretically (see Kitajima *et al* (2000), and the work cited therein). Schulz (1961) measured dissociative electron attachment to N₂O and observed a band at 2.3 eV with a small shoulder on the low-energy side. Chantry (1969) measured the dissociative attachment spectra at temperatures ranging from about 160 to 1000 K and showed that the low-energy shoulder rose dramatically with temperature. He also measured the O⁻ kinetic energy release using a Wien filter. The dramatic temperature dependence was explained by Bardsley (1969) in terms of qualitative potential curves. His assumptions about the potential curves of the negative ion were confirmed by the calculations of Hopper *et al* (1976). Dissociative electron attachment to condensed N₂O was measured by Bass *et al* (1997) who also presented a detailed account of the history of the problem. Brüning *et al* (1998) remeasured the temperature dependence and measured kinetic energy release by time-of-flight. Tronc *et al* (1977) measured the angular dependence of the differential cross section for O⁻ formation and found a minimum around 90°. Andrić and Hall (1984) measured the angular distribution of inelastically scattered electrons in the 1.4–3.1 eV range and at the 8 eV resonance. They concluded that a broad Σ resonance is present around 1.8 eV and a Π resonance around 2.4 eV. Angular distribution at the 8 eV resonance indicated Σ symmetry. Absolute elastic and vibrationally inelastic differential cross sections have been measured in the range 1.5–100 eV and 15°–130° by Kitajima *et al* (1999, 2000). Akhter *et al* (2002) measured the temperature dependence of scattered signal and derived the cross sections (at 2.5 eV) from the (010) excited vibrational state. Sarpal *et al* (1996a, 1996b), Morgan *et al* (1997) and Tennysson and Morgan (1999) calculated elastic cross sections using the *R*-matrix theory. Winstead and McKoy (1998) calculated elastic cross sections with the Schwinger multichannel (SMC) method including polarization, and da Costa and Bettge (1998) at the static exchange approximation with the SMC method with pseudopotentials. The present study investigates whether vibrational Feshbach resonances affect vibrational excitation and dissociative electron attachment near threshold in N₂O. A preliminary account of this work was given by Hotop *et al* (2003). Elastic and vibrational excitation cross sections are also presented at higher energies up to 12 eV.

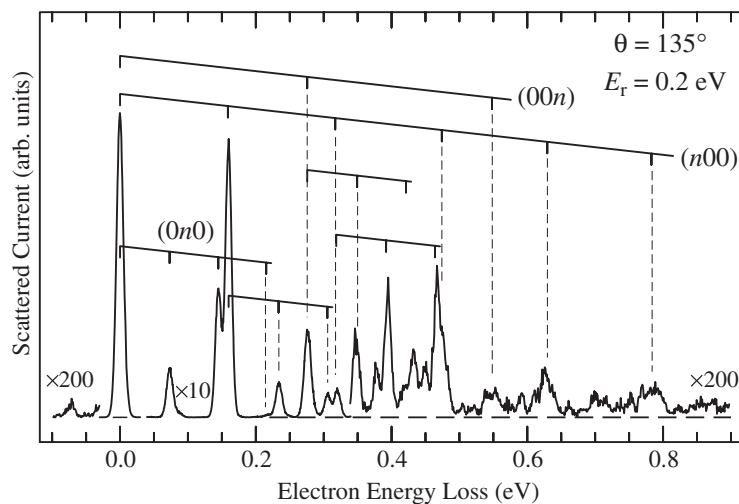


Figure 1. Energy loss spectrum of N_2O recorded at a constant residual energy close to threshold.

2. Experiment

The measurements were performed using a spectrometer with hemispherical analysers described by Allan (1992, 1995). The elastic peak in figure 1 is 12 meV wide, indicating a resolution of 12 meV in the energy loss spectrum, that is about 8.5 meV in the incident electron beam. The beam currents were 100–200 pA. The energy of the incident beam was calibrated on the 19.365 eV (Gopalan *et al* 2003) ^2S resonance in helium and is accurate to within ± 20 meV. The response function of the spectrometer was determined on the elastic scattering in helium.

The absolute value of the elastic cross section was determined by comparison with the elastic cross section of helium of Nesbet (1979) using the relative flow method. The gases were introduced through a single nozzle with a 0.25 mm diameter, made of molybdenum and kept at $\sim 30^\circ\text{C}$ during the measurements. The measurements were performed at several backing pressures ranging from 0.05 to 0.2 mbar, verifying that the result does not significantly depend on pressure. The inelastic cross sections were normalized to the elastic cross section and are accurate to within $\pm 30\%$ (less accurate within the first 100 meV above threshold). The present experiments were performed at various pressures to ascertain that the observed structures are not due to clusters, where vibrational Feshbach resonances have recently been observed by Weber *et al* (1999) and Leber *et al* (2000).

3. Results and discussion

3.1. Elastic scattering and vibrational excitation

The energies of the fundamental vibrational states of N_2O are 159.3 meV (ν_1 , ‘symmetric’, primarily N–O stretch), 73.0 meV (ν_2 , bend), and 275.7 meV (ν_3 , ‘asymmetric’, primarily $\text{N}\equiv\text{N}$ stretch) (Smith and Overend 1972). Many of the vibrational states are affected by Fermi resonances, that is, they undergo mixing due to anharmonicity of the potentials. Affected are for example the (10^0) and the (02^0) levels (Herzberg 1945), but the resulting mixing is less dramatic than in CO_2 because the separation Δ_0 of the unperturbed states is much larger (Grosso and McCubbin 1964).

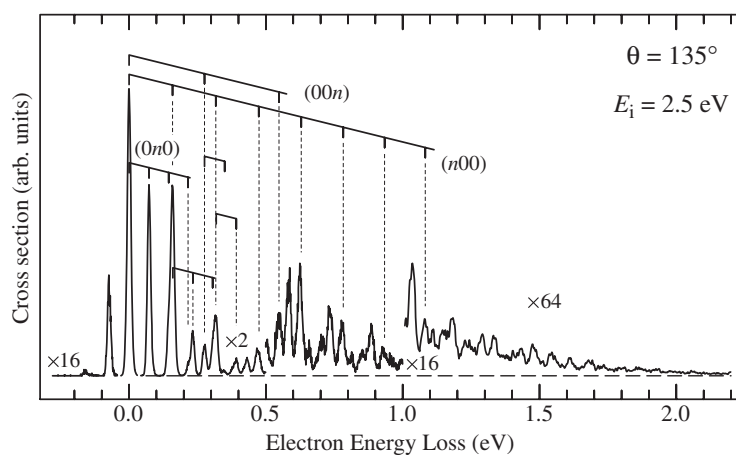


Figure 2. Energy loss spectrum of N_2O recorded at a constant incident energy within the ${}^2\Pi$ resonance.

The energy loss spectrum in figure 1 has been recorded at a constant low residual energy and characterizes excitation processes near threshold. All three modes are active and, in comparison to CO_2 , more excitation of overtone and combination vibrations occurs. The energy loss spectrum in figure 2 has been recorded at a constant incident energy and characterizes excitation processes via the ${}^2\Pi$ resonance. It resembles the spectrum obtained by Azria *et al* (1975) at 40° , interpreted theoretically by Dubé and Herzenberg (1975). All three modes, but primarily the N–O stretch, are active. Very strong excitation of overtone and combination vibration occurs, characteristic of a shape resonance and similar to the ${}^2\Pi_u$ resonance of CO_2 .

The vibrationally elastic cross section shown in figure 3 rises rapidly at low energies. The elastic cross section at 135° is lower in N_2O than in CO_2 , the former being $0.67 \text{ \AA}^2 \text{ sr}^{-1}$, the latter $2.8 \text{ \AA}^2 \text{ sr}^{-1}$ at 100 meV (Allan 2002). This is in line with previous experiments and theoretical predictions, which found the CO_2 cross section to be enhanced by a virtual state (Morrison 1982, Morgan *et al* 1997, Field *et al* 2001). The N_2O cross section was found to rise faster toward lower energies than the CO_2 cross section in the present study, however, reaching the value of $2 \text{ \AA}^2 \text{ sr}^{-1}$ at 30 meV. The difference between N_2O and CO_2 thus appears to be smaller at very low energies. Although integral cross sections were not measured in the present work, the present data at very low energies appear to be larger than the predictions of Sarpal *et al* (1996a, 1996b) and Winstead and McKoy (1998), and compatible with those of Morgan *et al* (1997).

The vibrationally inelastic cross sections shown in figures 3–5 reveal a close phenomenological similarity to CO_2 . The cross sections for the excitation of the fundamental vibrations are structureless (or nearly so—very weak structure appears in the excitation of the (100) vibration N_2O) in both N_2O and CO_2 , but structures appear in the excitation of overtones. The structure in N_2O is generally more pronounced than in CO_2 . The detailed shape and depth of the structures as well as the height of the threshold peaks depend strongly on the final vibrational state—they are surprisingly weak in the (020) and the (110) channels. In analogy with CO_2 the near-threshold structures can be assigned to vibrational Feshbach resonances supported by an electronic state of N_2O^- with a spatially diffuse electron wavefunction. The spacings of the structures indicate activity of the bending and the N–O stretch vibrations (figure 6).

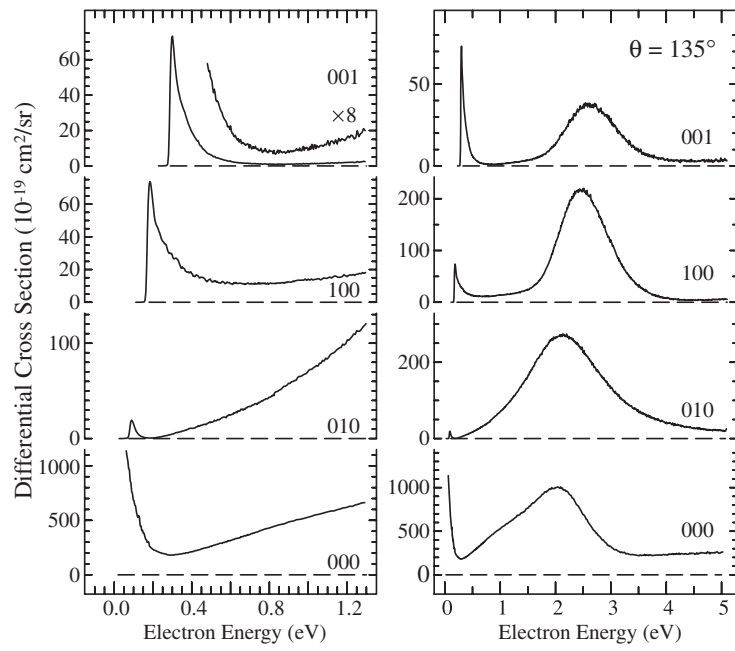


Figure 3. Differential cross sections for the elastic scattering and the excitation of the fundamental vibrations in N_2O . Detail of the threshold region is shown on the left, a wider energy range on the right.

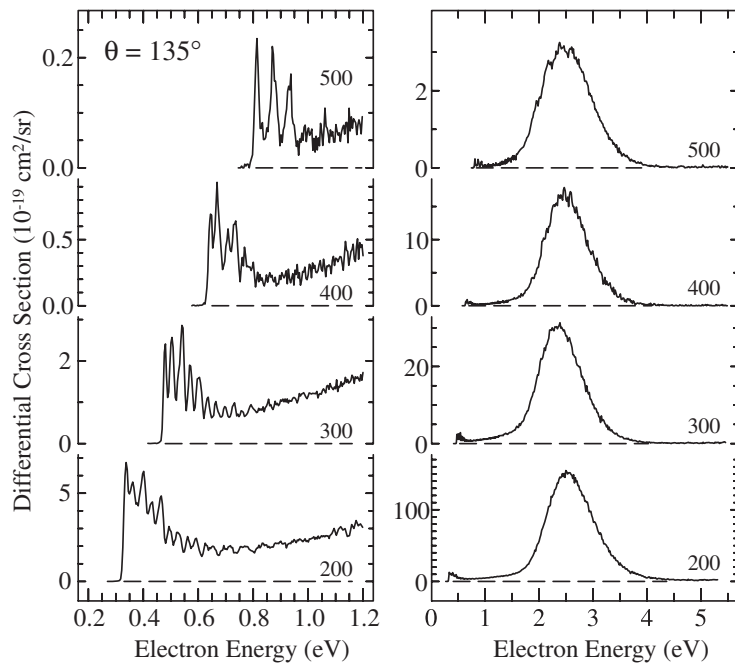


Figure 4. Differential cross sections for the excitation of the overtones of the N–O stretch vibration in N_2O . Detail of the threshold region is shown on the left, a wider energy range on the right.

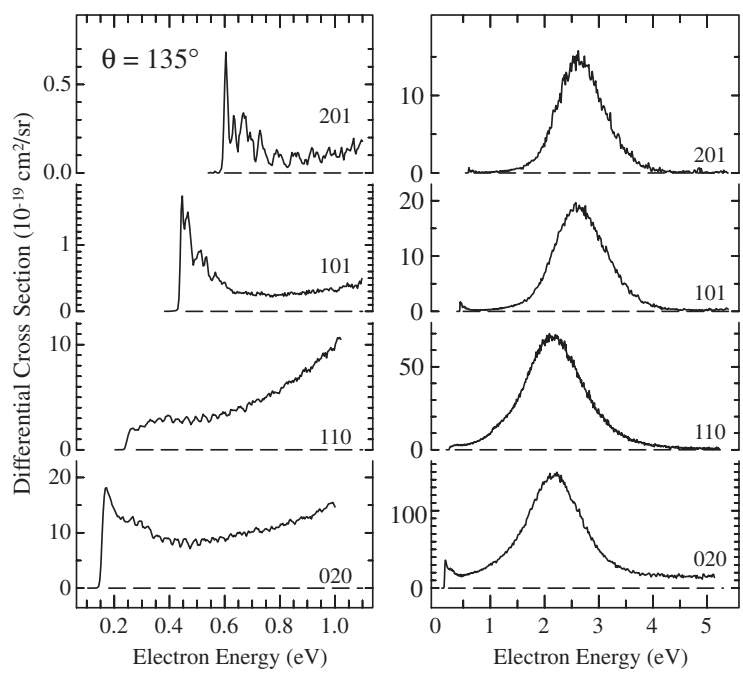


Figure 5. Differential cross sections for the excitation of overtone and combination vibrations in N_2O . Detail of the threshold region is shown on the left, a wider energy range on the right.

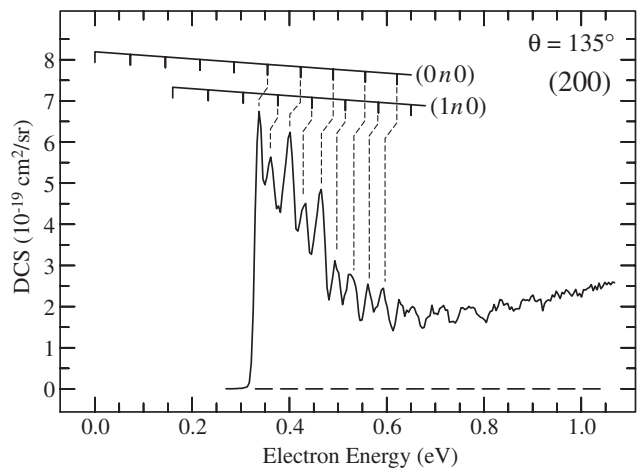


Figure 6. Enlarged view of the cross section for exciting the (200) level. Vibrational energies of neutral N_2O are indicated by grids.

The boomerang structures in the $^2\Pi$ region are much less pronounced than in CO_2 . They appear only weakly and only in a very high final channel, the excitation of the (500) state.

3.2. Dissociative electron attachment

The low threshold to dissociative electron attachment permits the study of the vibrational Feshbach resonances in the dissociative channel, as shown in figure 7. The spectra were recorded with the same spectrometer and the same resolution in the incident beam as all other

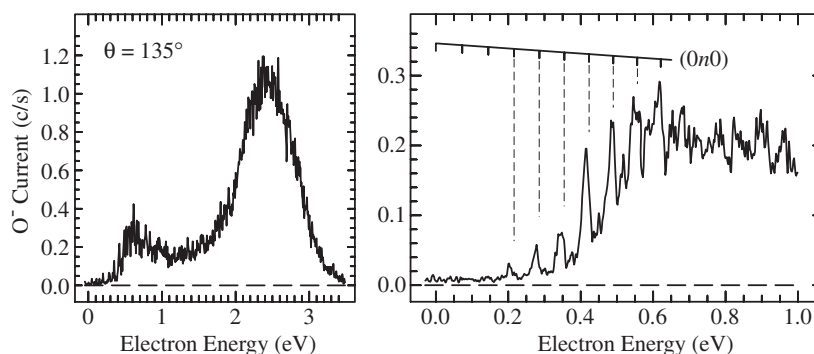


Figure 7. Dissociative electron attachment spectra. A wide energy range is shown on the left, and a detailed view of the low-energy region on the right. A progression of the bending vibration of neutral N_2O is indicated by a grid.

spectra in this paper. A small Wien filter separated electrons and ions. The only energetically open channel is the production of O^- ions. The spectrometer collects only one specific ion energy. The analyser setting was varied during the scan to collect ions whose energy was always about 25% of the maximum energy permitted by momentum conservation. The fact that only ions with one specific kinetic energy were collected resulted in very low signal levels.

The spectrum on the left closely resembles the spectra of Schulz (1961), Chantry (1969), Krishnakumar and Srivastava (1990) and Brüning *et al* (1998). The detail of the spectrum on the right reveals that what initially appeared as a continuous band consists in reality of narrow peaks whose spacings and positions are related to the bending vibration of N_2O . The peaks are observed 10 ± 20 meV below the vibrational levels; the difference is less than the error bar. It thus appears that the mechanism of dissociative electron attachment in N_2O at low energies is more complex than a simple dissociation of a repulsive shape resonance. The vibrational Feshbach resonances act as ‘doorway states’ and then predissociate into the dissociative continuum. Peaks in dissociative electron attachment ascribed to vibrational Feshbach resonances were already observed in CH_3I by Schramm *et al* (1999) and predicted theoretically for CH_3Cl and CH_3Br by Wilde *et al* (2000). Another precedent is the low-energy dissociative electron attachment to the strongly polar molecule ethylene carbonate, interpreted as dissociation of a vibrationally excited dipole bound state by Stepanović *et al* (1999). Individual vibrational Feshbach resonances were not resolved there, however. Sommerfeld (2002) discussed the role of vibrational Feshbach resonances as doorway states from the theoretical point of view in nitromethane.

The threshold energy for dissociative electron attachment, derived from the NN–O dissociation energy of 1.67 eV (Kaufman 1967) and the electron affinity of the O atom, 1.46 eV, is 0.21 eV. Brüning *et al* (1998) measured the temperature dependence of the O^- signal and concluded that the activation barrier of dissociative attachment is 0.213 ± 0.042 eV, which corresponds to the thermodynamic threshold of the reaction. In contrast, Kryachko *et al* (2001) calculated a barrier of about 0.5 eV, in agreement with an earlier experimental value of Wentworth *et al* (1971). The lowest discernable peak in the right panel of figure 7 is at 0.21 eV, but a conclusion concerning the height of the activation barrier is not possible because the low-lying peaks in figure 7 could be, at least in part, hot bands. Chantry (1969) measured spectra at low temperatures and found the signal in the 0.2–1.5 eV range to decrease with decreasing temperature even well below room temperature. This indicates that part, but not all, of the signal in this energy range is due to hot bands even at room temperature. An immensely rapid

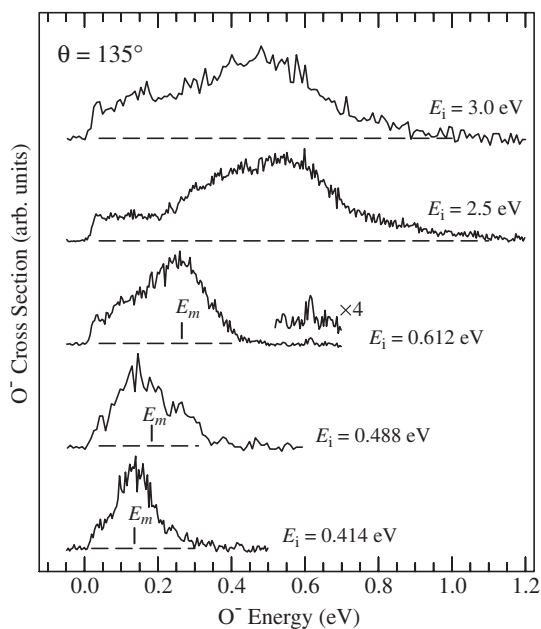


Figure 8. O⁻ kinetic energy distributions for the incident electron energies E_i given. The maximum possible O⁻ energies from dissociative electron attachment to ground state N₂O are marked by vertical bars labelled E_m . The values at $E_i = 2.5$ and 3.0 eV are outside of the figure, at 1.46 and 1.78 eV respectively.

increase of the cross section with the vibrational quantum would be required to explain the 0.21 eV O⁻ peak as a hot band with an activation barrier of 0.5 eV, however. High-resolution experiments with cooled N₂O would be desirable to resolve this issue.

O⁻ kinetic energy distributions were measured by sweeping the analyser setting for a fixed incident electron energy and using the Wien filter to separate ions from scattered electrons. (A weak peak due to elastically scattered electrons which were not entirely eliminated by the Wien filter can be discerned in the spectrum with $E_i = 0.612$ eV. It allows us to determine the rejection efficiency of the Wien filter as about 50 000.) The spectra were then corrected by assuming the same response function as for collecting electrons. The results are shown in figure 8. The curves peak at energies somewhat higher than the mean values reported by Brüning *et al* (1998). The present mean energy at $E_i = 0.612$ eV, calculated from the spectrum in figure 8, is 0.23 eV, compared to 0.14 eV reported by Brüning *et al* (1998). At $E_i = 2.5$ eV the present value is 0.50 eV, compared to 0.22 eV of Brüning *et al* (1998). The present distribution at $E_i = 3.0$ eV peaks slightly below (mean energy 0.44 eV) that at $E_i = 2.5$ eV, confirming the finding of Brüning *et al* (1998) that the mean O⁻ kinetic energy drops at incident energies above about 2.5 eV. The present curves are in remarkable agreement with those published 34 years ago by Chantry (1969). Thus the present distribution at $E_i = 0.612$ eV peaks at 0.255 eV, in agreement with Chantry's curve at $E_i = 0.75$ eV which peaks at about 0.25 eV. Chantry's curve at $E_i = 2.5$ eV peaks around 0.4 eV as compared to the present value of about 0.5 eV—also a very good agreement in view of the very flat top of the peak. The present ion energies are also in a good agreement with the values measured by Schulz (1961) using ion retardation. The high values of kinetic energies obtained with low incident energies are somewhat puzzling. The maximum O⁻ kinetic energy

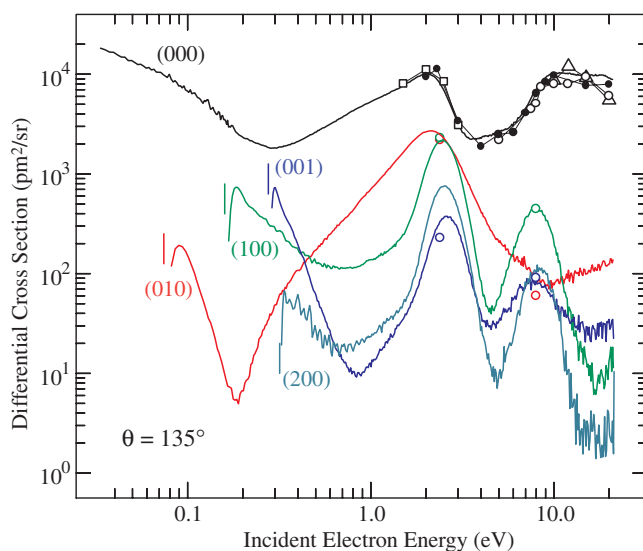


Figure 9. Differential elastic and selected vibrational cross sections on a log–log scale. The elastic data of Marinković *et al* (1986) are shown by triangles. The elastic data of Johnstone and Newell (1993), extrapolated to 135° from their data at 120°, are shown as empty circles. The elastic data of Kitajima *et al* (2000), extrapolated to 135° from their data at 130°, are shown as empty squares (Sophia University data) and filled circles (Australian National University data). The vibrationally inelastic data of Kitajima *et al* (2000), extrapolated to 135°, are shown as empty circles (note that their data for the (010) and the (100) states nearly coincide at 2.4 eV and the two circles overlap).

given by momentum conservation, obtained with $E_i = 0.414$ eV and a thermodynamic limit of 0.2 eV, would be $E_{\max} = (0.414 - 0.2) \times 28/44 = 0.14$ eV—much less than the observed maximum energy of about 0.25 eV. Figure 8 shows that the same discrepancy is encountered at $E_i = 0.488$ and 0.612 eV. This fact was already remarked by Chantry (1969) although the lower resolution of his experiment made the observation less striking—Chantry compared the peak values and not the high-energy onsets with the theoretical maximum energies. Chantry explained the high kinetic energies as a consequence of attachment to vibrationally excited N_2O molecules and this interpretation remains viable since the only alternative, an assumption that the NN–O dissociation energy is less than 1.67 eV (an explanation considered by Schulz 1961), appears unacceptable in view of the strong arguments brought in favour of this value by Kaufman (1967).

The ion energy distribution curves show no structures at the openings of the channels leading to a vibrationally excited fragment $\text{N}_2(v)$. This indicates substantial rotational excitation, compatible with the assumption that the transition state of N_2O^- is bent.

3.3. Scattering at energies up to 12 eV

Figure 9 shows the differential cross sections from near threshold until 12 eV on a log–log scale. The present values of the cross sections agree well with those of Marinković *et al* (1986), Johnstone and Newell (1993) and of Kitajima *et al* (2000). The comparison of the theoretical and the experimental elastic cross sections above 1.5 eV has been discussed in detail by Kitajima *et al* (2000). The latter paper presented two data sets, from the Sophia University and the Australian National University. The two data sets are mutually consistent and only the latter set is shown at higher energies to avoid congestion of figure 9. Only one resonance,

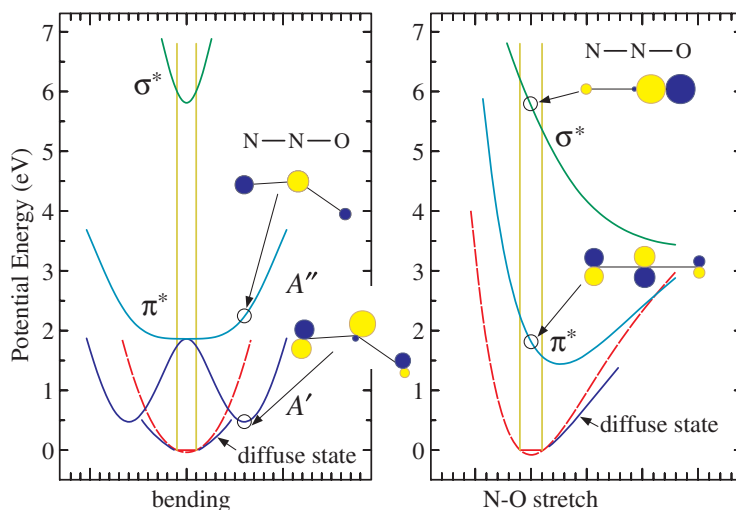


Figure 10. Qualitative potential curves of N_2O (dashed) and its anion. Qualitative diagrams of the virtual orbitals are shown both at linear and bent geometries. (Drawn with the program MOPLOT, Bally and Olkhov 2003.)

at 8 eV, already studied experimentally by Andrić and Hall (1984), can be discerned at higher energies. The vibrational excitation at 8 eV is selective, a band appears clearly in the N–O stretch cross sections (100) and (200), weaker in the $\text{N}\equiv\text{N}$ stretch cross section (001), and is absent in the bending excitation cross section (010). This selectivity indicates a $\sigma_{\text{N-O}}^*$ shape resonance. This conclusion is consistent with the finding of Andrić and Hall (1984) that this resonance has Σ symmetry, as well as with the calculation of Winstead and McKoy (1998) who obtained an indication of a Σ resonance in the form of a step in the ${}^2\Sigma + {}^2\Delta$ eigenphase sum around 8 eV.

3.4. Qualitative potential curves

We used the Koopmans model (Koopmans 1934) with empirical scaling (Chen and Gallup 1990) to approximate the real part of the anion potential curves. We took the Hartree–Fock self-consistent field energy as a function of the normal coordinate to approximate the potential curve of the neutral molecule and added the scaled virtual orbital energies to obtain the potential curves of the anion as described in more detail for chlorobenzene by Skalický *et al* (2002). For consistency with our earlier work we use the 6-31G* basis set and the scaling parameters of Chen and Gallup (1990). The use of this very simple model is justified by its success in reproducing qualitatively or semiquantitatively the energies of shape resonances in widely diverging molecules, not only the π^* states of conjugated hydrocarbons on which the empirical scaling was primarily calibrated, but also π^* and/or σ^* states in, for example, propellane (Schafer *et al* 1992), allene (Allan 1994), cyclopropane (Allan and Andrić 1996), chlorobenzene (Skalický *et al* 2002) and ozone (Allan and Popović 1997).

Figure 10 shows the curves as a function of the bending and N–O stretch vibrational coordinates. The π^* attachment energy is calculated at 1.9 eV, in reasonable agreement with the experimental value of 2.3 eV. The next higher shape resonance is predicted to be a σ^* state calculated around 6 eV. The wavefunction is localized on, and is antibonding with respect to, the N–O bond, resulting in a large slope of the surface along the N–O stretch coordinate.

This σ^* resonance is thus predicted to excite primarily the N–O stretch vibration, less the N \equiv N vibration, and be absent in the bending excitation. These properties fit well the resonance observed at 8 eV in the spectra and we therefore consider it a viable assignment, although the difference of the measured and calculated values is larger than in the cases cited above. The π^* resonance splits into A' and A'' components upon bending and has a slope with respect to the N–O stretch (as already noted by Hopper *et al* 1976), rationalizing its prominence in the bending and N–O stretch excitation cross sections. We do not obtain evidence for a low-lying σ^* resonance sometimes postulated in the 1.5–2.5 eV range (apart from the fact that the A' branch of the π^* resonance would be considered to be ' σ^* ' in chemical terms for the bent anion).

The structure due to vibrational Feshbach resonances reported here shows activity of the N–O stretch and the bending vibrations. We therefore propose that an adiabatic potential surface of a spatially diffuse dipole and polarization bound state of the anion is found below the neutral potential surface for molecules distorted along these coordinates, as shown schematically in figure 10.

4. Conclusions

The findings on vibrational excitation cross sections in N₂O near threshold resemble those in CO₂. Narrow structures with spacings nearly identical to bending and N–O stretch vibrational frequencies of neutral N₂O are found in the excitation of many overtone vibrations. The structures become deeper and more pronounced in the cross sections for the excitation of higher overtones. Since the ² Π shape resonance is at a substantially higher energy, an explanation of the threshold structures analogous to that in CO₂ is favoured—as vibrational Feshbach resonances supported by a 'diffuse state' of the anion, where an electron is loosely bound by a combination of polarization forces and a dipolar force of a vibrating N₂O. The elastic cross section is found to dramatically increase at low energies.

Structures with the spacings of the bending vibration of neutral N₂O are also found in the dissociative electron attachment. They are assigned to the same vibrational Feshbach resonances, predissociated by the A' valence state. The lowest O⁻ peak is at 0.21 eV, but this does not prove the absence of a barrier to dissociation because hot bands appear to make a substantial contribution to the sharp peaks observed in the dissociative attachment spectrum even at room temperature.

Acknowledgment

This research is part of project no 2000-067877.02 of the Swiss National Science Foundation.

References

- Akhter P, Johnstone W M, El-Zein A A A, Campbell J, Teubner P J O, Brunger M J and Newell W R 2002 *J. Phys. B: At. Mol. Opt. Phys.* **35** L481
- Allan M 1992 *J. Phys. B: At. Mol. Opt. Phys.* **25** 1559
- Allan M 1994 *J. Chem. Phys.* **100** 5588
- Allan M 1995 *J. Phys. B: At. Mol. Opt. Phys.* **28** 5163
- Allan M 2001 *ICPEAC: 22nd Int. Conf. on the Photonic Electronic and Atomic Collisions (Santa Fe, NM)* p 275 (Abstracts of contributed papers)
- Allan M 2002 *J. Phys. B: At. Mol. Opt. Phys.* **35** L387–95

- Allan M 2003 *J. Phys. B: At. Mol. Opt. Phys.* **36** 2489
- Allan M and Andrić L 1996 *J. Chem. Phys.* **105** 3559
- Allan M, Čížek M, Horáček J and Domcke W 2000 *J. Phys. B: At. Mol. Opt. Phys.* **33** L209
- Allan M and Popović D B 1997 *Chem. Phys. Lett.* **268** 50
- Alms G R, Burnham A K and Flygare W H 1975 *J. Chem. Phys.* **63** 3321
- Andrić L and Hall R I 1984 *J. Phys. B: At. Mol. Phys.* **17** 2713
- Azria R, Wong S F and Schulz G J 1975 *Phys. Rev. A* **11** 1309
- Bally T and Olkhov R 2003 The program MOPLLOT <http://www-chem.unifr.ch/frames/facilities/moplot/moplot.html>
- Bardsley J N 1969 *J. Chem. Phys.* **51** 3384
- Bass A D, Lezius M, Ayotte P, Parenteau L, Cloutier P and Sanche L 1997 *J. Phys. B: At. Mol. Opt. Phys.* **30** 3527
- Brüning F, Matejčík S, Illenberger E, Chu Y, Senn G, Muigg D, Denifl G and Märk T D 1998 *Chem. Phys. Lett.* **292** 177
- Chantry P J 1969 *J. Chem. Phys.* **51** 3369
- Chen D and Gallup G A 1990 *J. Chem. Phys.* **93** 8893
- Christophorou L G, McCorkle D L and Christodoulides A A 1984 *Electron-Molecule Interactions and Their Applications* vol 1, ed L G Christophorou (New York: Academic) ch 6, p 569
- Čížek M, Horáček J, Allan M and Domcke W 2002 *Czech. J. Phys.* **52** 1057
- Čížek M, Horáček J, Allan M, Fabrikant I I and Domcke W 2003 *J. Phys. B: At. Mol. Opt. Phys.* **36** 2837
- Čížek M, Horáček J, Allan M, Sergenton A-C, Popović D B, Domcke W, Leininger T and Gadea F X 2001 *Phys. Rev. A* **63** 062710
- Cvejanović S 1993 *ICPEAC: 18th Int. Conf. on Physics of Electronic and Atomic Collisions (Aarhus, 1993) (AIP Conf. Proc. vol 295)* ed T Andersen, B Fastrup, F Folkmann, H Knudsen and N Anderson (New York: American Institute of Physics) p 390
- Cvejanović S and Jureta J 1989 *3rd Eur. Conf. on At. Mol. Phys. (Bordeaux)* p 638 (Abstracts)
- da Costa S M S and Bettiga M H F 1998 *Eur. Phys. J. D* **3** 67
- Dubé L and Herzenberg A 1975 *Phys. Rev. A* **11** 1314
- Field D, Jones N C, Lunt S L and Ziesel J P 2001 *Phys. Rev. A* **64** 022708
- Gopalan A, Bömmels J, Götze S, Landwehr A, Franz K, Ruf M-W, Hotop H and Bartschat K 2003 *Eur. Phys. J. D* **22** 17
- Grosso R P and McCubbin T K Jr 1964 *J. Mol. Spectrosc.* **13** 240
- Herzberg G 1945 *Molecular spectra and molecular structure Infrared and Raman Spectra of Polyatomic Molecules* vol 2 (Princeton, NJ: Van Nostrand-Reinhold) p 277
- Hopper D G, Wahl A C, Wu R L C and Tierman T O 1976 *J. Chem. Phys.* **65** 5474
- Hotop H, Ruf M-W, Allan M and Fabrikant I I 2003 *Adv. At. Mol. Opt. Phys.* at press
- Jalink H, Parker D H and Stolte S 1987 *J. Mol. Spectrosc.* **121** 236
- Johnstone W M and Newell W R 1993 *J. Phys. B: At. Mol. Opt. Phys.* **26** 129
- Jones N C, Field D, Ziesel J-P and Field T A 2002 *Phys. Rev. Lett.* **89** 093201
- Kaufman F 1967 *J. Chem. Phys.* **46** 2449
- Kitajima M, Sakamoto Y, Gully R J, Hoshino M, Gibson J C, Tanaka H and Buckman S J 2000 *J. Phys. B: At. Mol. Opt. Phys.* **33** 1687
- Kitajima M, Sakamoto Y, Watanabe S, Suzuki T, Ishikawa T, Tanaka H and Kimura M 1999 *Chem. Phys. Lett.* **309** 414
- Knott G, Gote M, Rädle M, Jung K and Ehrhardt H 1989 *Phys. Rev. Lett.* **62** 1735
- Kochem K-H, Sohn W, Hebel N, Jung K and Ehrhardt H 1985 *J. Phys. B: At. Mol. Phys.* **18** 4455
- Koopmans T 1934 *Physica A* **104** 1
- Krishnakumar E and Srivastava S K 1990 *Phys. Rev. A* **41** 2445
- Kryachko E S, Vinckier C and Nguyen M T 2001 *J. Chem. Phys.* **114** 7911
- Leber E, Barsotti S, Bömmels J, Weber J M, Fabrikant I I, Ruf M-W and Hotop H 2000 *Chem. Phys. Lett.* **325** 345
- Lide D R (ed) 1995 *CRC Handbook of Chemistry and Physics* 76th edn (Boca Raton, FL: Chemical Rubber Company Press)
- Marinković B, Szymkowski C, Pejčev V, Filipović D and Vušković L 1986 *J. Phys. B: At. Mol. Phys.* **19** 2365
- Morgan L A, Gillan C J, Tennysson J and Chen X 1997 *J. Phys. B: At. Mol. Opt. Phys.* **30** 4087
- Morrison M A 1982 *Phys. Rev. A* **25** 1445
- Nesbet R K 1979 *Phys. Rev. A* **20** 58
- Rohr K and Linder F 1976 *J. Phys. B: At. Mol. Phys.* **9** 2521
- Sarpal B K, Pflingst K, Nestmann B M and Peyerimhoff S D 1996a *J. Phys. B: At. Mol. Opt. Phys.* **29** 857
- Sarpal B K, Pflingst K, Nestmann B M and Peyerimhoff S D 1996b *J. Phys. B: At. Mol. Opt. Phys.* **29** 1877 (corrigendum)
- Schafer O, Allan M, Szeimies G and Sanktjohanser M 1992 *J. Am. Chem. Soc.* **114** 8180

Schramm A, Fabrikant I I, Weber J M, Leber E, Ruf M-F and Hotop H 1999 *J. Phys. B: At. Mol. Opt. Phys.* **32** 2153
Schulz G J 1961 *J. Chem. Phys.* **34** 1778
Skalický T, Chollet C, Pasquier N and Allan M 2002 *Phys. Chem. Chem. Phys.* **4** 3583
Smith D F and Overend J 1972 *Spectrochim. Acta A* **28** 87
Sommerfeld T 2002 *Phys. Chem. Chem. Phys.* **4** 2511
Stepanović M, Pariat Y and Allan M 1999 *J. Chem. Phys.* **110** 11376
Tennysson J and Morgan L 1999 *Phil. Trans. R. Soc. A* **357** 1161
Tronc M, Fiquet-Fayard F, Schermann C and Hall R I 1977 *J. Phys. B: At. Mol. Phys.* **10** L459
Weber J M, Leber E, Ruf M-W and Hotop H 1999 *Phys. Rev. Lett.* **82** 516
Wentworth W E, Chen E and Freeman R 1971 *J. Chem. Phys.* **55** 2075
Wilde R S, Gallup G A and Fabrikant I I 2000 *J. Phys. B: At. Mol. Opt. Phys.* **33** 5479
Winstead C and McKoy V 1998 *Phys. Rev. A* **57** 3589